Springer

Acta Mechanica Sinica

CrossMark click for updates

• RESEARCH PAPER •

Acta Mech. Sin., Vol. 41, 424352 (2025)
https://doi.org/10.1007/s10409-024-24352-x

Boussinesq problem of a finite elastic layer with the surface effect

Hui Wu[1], Sha Xiao[1], Zhilong Peng[1], Ning Jia[2*], and Shaohua Chen[1*]

[1] *School of Aerospace Engineering, Beijing Institute of Technology, Beijing 100081, China;*
[2] *Department of Applied Mechanics, University of Science and Technology Beijing, Beijing 100083, China*

Received June 6, 2024; accepted August 13, 2024; published online November 21, 2024

Both the thickness effect and surface effect should be important in nano-indentation behavior of coatings due to the finite thickness and small indentation size. As a basic solution, the two-dimensional Boussinesq problem of a finite elastic layer bonded to a rigid substrate is studied in this paper, employing the surface-energy-density-based elastic theory. The Airy stress function and Fourier integral transform methods are adopted to solve the problem. A nalytical solutions of both the stress and displacement fields are well achieved for a finite elastic layer under a concentrated force and a uniform pressure. Unlike the classical solutions, it is discovered that both the thickness effect and surface effect will show significant influences on the Boussinesq elastic behaviors. The surface effect would harden the finite elastic layer and induce a more uniformly distributing displacements and stresses. Only when the thickness is sufficiently large, the Boussinesq solution of an elastic half space may represent that of a finite elastic layer case. A generalized hardness is further defined to include the coupling effects of thickness and surface for the Boussinesq problem of a finite elastic layer. Such a study would assist in the design and property evaluation of coatings and micro-devices with layer-substrate structures.

Boussinesq problem, Finite elastic layer, Surface effect, Thickness effect, Analytical solution

Citation: H. Wu, S. Xiao, Z. Peng, N. Jia, and S. Chen, Boussinesq problem of a finite elastic layer with the surface effect, Acta Mech. Sin. 41, 424352 (2025), https://doi.org/10.1007/s10409-024-24352-x

1. Introduction

Nanoindentation, as an advanced nanotechnology, is widely used for the mechanical property characterization (elastic modulus, hardness, and yield stress, etc.) of various materials, such as crystal, electromechanical smart materials, biocompatible materials with compound microstructures and thin films [1-4]. Interestingly, when the indentation size or material dimension is reduced to the micro/nanoscale, the indentation hardness shows a significant size dependence [5,6]. Particularly for indentation depths or indenting width (radius) smaller than 100 nm, both atomic simulation [7] and experimental evaluation [8] have demonstrated the prominent impact of the surface effect on contact problem, which is ascribed to the increasing of the ratio of surface to volume [9-11]. However, the classical theory cannot explain and predict such an effect.

In the 1970s, a rigorous mathematical framework, by introducing surface residual stresses and surface elastic constants, had established to depict the material's surface effect by Gurtin and Ian Murdoch [12,13]. As the assumption, the surface is considered a two-dimensional thin film without thickness, the deformation is continuous between the surface and bulk. The linear elastic constitutive relation still applies to the mechanical behavior of the surface. Subsequently, several extensive models derived from the Gurtin and Murdoch (G-M) theory have been put forward. Dingreville and Qu [14] introduced the surface free energy to describe the surface effect. Steigmann and Ogden [15] proposed a constitutive model, which introduces a surface flexural stiffness, to predict the behavior of bending or wrinkling of nanowires (NWs) incorporating the surface effect. Huang and Wang [16] introduced a surface hyperelastic theory that

*Corresponding authors. E-mail addresses: jianing@ustb.edu.cn (Ning Jia); shchen@bit.edu.cn (Shaohua Chen)
Executive Editor: Haimin Yao

© The Chinese Society of Theoretical and Applied Mechanics and Springer-Verlag GmbH Germany, part of Springer Nature 2024

accounted for the interfacial energy and internal residual stress. Wang et al. [17] adopted the surface residual stress to describe the size-dependent surface in nanomaterials. The G-M theory and its expansions have been well used to analyze the surface effect on many nanostructures and nanomaterials [18-27].

Recently, many researchers concerned about the nanocontact problems by the G-M theory [28-32]. The first category relates to the nanocontact issue with a semi-infinite plane. Gao et al. [30] examined the Boussinesq problem on semi-infinite plane incorporating surface residual stress, in which it was found that the deformation of the semi-infinite plane is smoother resulted from hardening effect induced by the surface effect. Subsequent studies extended this analysis to the contact behaviors of two typical nano-indenters of a semi-infinite plane by Long et al. [33]. The second category is the nanocontact issue of structures with a finite thickness. Zhao and Rajapakse [34] studied the nanocontact behavior on an elastic layer using the G-M theory. Examining the contact problem by introducing the surface tension on an elastic dhered layer using G-M theory, Yuan and Wang [29] discovered that the surface tension significantly increased the elasticity of the elastic layer, resulting in a more consistent contact pressure. Attia and Mahmoud [35] studied how the surface elastic constants affect the contact behavior of a finite-thickness functionally graded substrate. Lawongkerd et al. [36] solved an elastic loading problem for a thin layer perfectly bonding to the rigid substrate.

In accordance with the G-M theory and its expansions, the contact models above modified the stress boundary conditions through adding the residual stress or elastic constants of surface. However, both kinds of parameters are difficult to obtain experimentally or yield precisely by the molecular dynamics simulations [37]. To prevent introduction of the two kinds of parameters above, Chen and Yao [38] introduced an alternative surface elastic theory based on the surface energy density of nanomaterials, where the surface relaxation parameter and the bulk-surface-energy-density were involved to represent surface effect. Such a theory [38] offers the advantage of easily acquiring the two key parameters either from material manuals or by simple experiment observations. Consequently, the expression for the surface-induced traction is based on the surface energy density instead of the surface stress associated with the surface elastic constants. Mechanical characteristics of different nanostructures have been successfully assessed using surface-energy-density-rooted elastic theory [39-42].

The contact problems of a half space under different loading conditions were also examined by surface-energy-density-rooted elastic theory. Jia et al. [43] and Wang et al. [44] analyzed the Hertz contact of a semi-infinite space, in which a notable surface effect was found while the contact width or radius was on a par with the material's intrinsic length. Wang [45] analyzed the Boussinesq problem of a semi-infinite plane and found a smoother transition of stresses at the loading edge. The contact problem subjected by normal triangular loading was also studied by Wang et al. [46], in which the hardening effect was obviously found on account of the surface effect.

However, the results with the semi-infinite assumption are definitely not applicable to structures with finite thickness [2,47-49]. According to surface-energy-density-rooted elastic theory, semi-analytical analysis for the frictionless contact of a graded film punched by a cylindrical indenter was carried out by Zhang et al. [50], and the contact pressures were predicted with the influence of surface effect, elastic modulus, film thickness. Until now, there is still little theoretical analysis on the mechanical behaviors of finite layers considering both the surface and thickness effects, though it is an important basic issue for film-substrate systems and related micro-devices.

In order to give the basic solutions to the above problem, this paper investigates a two-dimensional Boussinesq model of a finite bonded elastic layer, using the surface-energy-density-rooted elastic theory [38]. Below is the outline of the paper. The surface elastic theory is briefly introduced in Sect. 2. The mathematical formula and general solutions considering the surface effect are given in Sect. 3. Then, analytical solutions for the Boussinesq problem of a finite boned elastic layer under a concentrated force or uniform pressure are achieved in Sect. 4. Section 5 gives the analysis of results and discussion. Conclusions are drawn finally, which would assist in the design of film-substrate systems and related micro-devices.

2. Brief introduction of the surface elastic theory

The surface theory established by Chen and Yao [38] rooted in surface energy density of nanostructures and nanomaterials is adopted in this work, which is briefly introduced in this section. Assuming a nano-material in a reference configuration with an idealized crystal structure, consider embedding a Lagrangian coordinate system on the solid surface, where its principal axes 1 and 2 align parallel to the basic vectors of the unit cell. In the reference configuration, the Lagrangian surface energy density ϕ^0 comprises two components: ϕ^0_{stru} associated with the surface strain energy and another ϕ^0_{chem} resulting from the surface chemical bond, i.e.,

$$\phi^0 = \phi^0_{\text{stru}} + \phi^0_{\text{chem}}, \tag{1}$$

$$\begin{cases} \phi_{\text{chem}}^{0} = \phi_{0b}\left(1 - w_1 \dfrac{D_0}{D}\right), \\ \phi_{\text{stru}}^{0} = \dfrac{E_b}{2\sin\beta} \displaystyle\sum_{i=1}^{2} a_{0i}\eta_i \left\{\left[3 - 3\left(\lambda_i + \lambda_i\varepsilon_{si}\right) + \left(\lambda_i + \lambda_i\varepsilon_{si}\right)^{-m}\right]\right. \\ \qquad \left. \times\left[\lambda_i^2\varepsilon_{si}^2 + \left(\lambda_i - 1\right)^2 + 2\lambda_i\left(\lambda_i - 1\right)\varepsilon_{si}\right]\right\}, \\ \qquad \eta_1 = \dfrac{a_{01}}{a_{02}},\ \eta_2 = \dfrac{a_{02}}{a_{01}}, \end{cases} \tag{2}$$

where ϕ_{0b} represents the bulk surface energy density. w_1 describes the scale-dependent behavior of ϕ_{chem}^{0} empirically, and D depicts the characteristic length of solid, which could be the thickness or diameter, and so on. D_0 is a length parameter ($D_0 = 2d_0$ for nanofilms, $D_0 = 3d_0$ for nanowires and nanoparticles, where d_0 is the atomic diameter). In the structural part ϕ_{stru}^{0}, E_b represents the bulk Young's modulus. The angle between the basic vectors is generally defined as $\beta = \pi/2$. $\lambda_i = a_{ri}/a_{0i}$ describes surface relaxation with the initial lattice length a_{0i} and surface relaxation lattice length a_{ri} in the crystal surface. $\varepsilon_{si} = (a_i - a_{ri})/a_{0i}$ represents the surface strain result from the external loading. The parameter m can depict the correlation between bond length and binding energy.

As for the deformation of nano-solid in the present configuration, the potential energy function Π is written as follows:

$$\begin{aligned} \Pi(\mathbf{u}) &= U + \Phi - W \\ &= \int_{V\text{-}S} \psi(\boldsymbol{\varepsilon})\mathrm{d}V + \int_S \phi(\boldsymbol{\varepsilon}_s)\mathrm{d}S - \int_{V\text{-}S} \mathbf{f}\cdot\mathbf{u}\mathrm{d}V - \int_{S_p} \mathbf{p}\cdot\mathbf{u}\mathrm{d}S, \end{aligned} \tag{3}$$

where the bulk elastic strain energy U, the surface free energy Ω and the external work W are concluded. ψ represents the elastic strain energy density, ϕ denotes the Eulerian surface energy density, $\mathbf{u}$ is the displacement, $\mathbf{f}$ is the body force, and $\mathbf{p}$ denotes the external surface traction. $\boldsymbol{\varepsilon}$ and $\boldsymbol{\varepsilon}_s$ are the strains in the bulk and the surface strains, respectively. S_p represents the boundary at which the external traction is acted.

The variational analysis [16,38] of Eq. (3) results in the equilibrium equations and the stress boundary conditions as follows:

$$\begin{cases} \boldsymbol{\sigma}\cdot\nabla + \mathbf{f} = \mathbf{0}, & (\text{in } V\text{-}S), \\ \mathbf{n}\cdot\boldsymbol{\sigma}\cdot\mathbf{n} = \mathbf{p}\cdot\mathbf{n} - \gamma_n, & (\text{on } S), \\ (\mathbf{I} - \mathbf{n}\otimes\mathbf{n})\cdot\boldsymbol{\sigma}\cdot\mathbf{n} = (\mathbf{I} - \mathbf{n}\otimes\mathbf{n})\cdot\mathbf{p} - \gamma_t, & (\text{on } S), \end{cases} \tag{4}$$

where $\mathbf{n}$ is the unit normal vector, $\mathbf{I}$ is a unit tensor, and $\boldsymbol{\sigma}$ is the bulk Cauchy stress tensor. Defining the additional traction induced by surface, i.e., the normal components γ_n and tangential components γ_t, which can be obtained by the virtual work method [38] as follows:

$$\begin{aligned} &\gamma_t = \nabla_s\phi = \frac{\nabla_s\phi_0}{J_s} - \frac{\phi_0(\nabla_s J_s)}{J_s^2}, \\ &\gamma_n\mathbf{n} = \phi\left(\frac{1}{R_1} + \frac{1}{R_2}\right)\mathbf{n} = \phi(\mathbf{n}\cdot\nabla_s)\mathbf{n}, \end{aligned} \tag{5}$$

where ∇_s acts as a surface gradient operator. Adopting $\phi = \phi_0/J_s$, where J_s denotes the Jacobean determinant related to the elements change from the configuration of Lagrangian to Eulerian. R_1 and R_2 denote the curvature radii for curved surface.

The handling of boundary conditions distinguishes the above surface elastic theory from the earlier frameworks [12,15,23,51]. In such a theory by Chen and Yao [38], the boundary conditions introduce the surface relaxation parameters and bulk surface energy density.

3. Boussinesq problem of a finite elastic layer considering surface effect

A two-dimensional finite elastic layer acted by the uniform pressure $p(x)$ on the surface is shown in Fig. 1. Assume a perfect bond between the elastic layer and a rigid substrate, and the pressure $p(x)$ is symmetrical about z-axis in the Cartesian coordinate system (xOz). The pressurized half-width is a and the thickness of layer is h. The plane strain condition yields $\varepsilon_{yx} = \varepsilon_{yy} = \varepsilon_{yz} = 0$.

3.1 Governing equations and boundary conditions

Without considering the body force, the equilibrium equations are written as follows:

$$\frac{\partial\sigma_x}{\partial x} + \frac{\partial\sigma_{xz}}{\partial z} = 0,\quad \frac{\partial\sigma_{xz}}{\partial x} + \frac{\partial\sigma_z}{\partial z} = 0, \tag{6}$$

where σ_x and σ_z denote the normal stresses, and σ_{xz} is the shear stress.

The geometric equation of the plane strain problem is

$$\varepsilon_x = \frac{\partial u_x}{\partial x},\quad \varepsilon_z = \frac{\partial u_z}{\partial z},\quad \varepsilon_{xz} = \frac{1}{2}\left(\frac{\partial u_x}{\partial z} + \frac{\partial u_z}{\partial x}\right), \tag{7}$$

where ε_x and ε_z denote the normal strains, and ε_{xz} is the

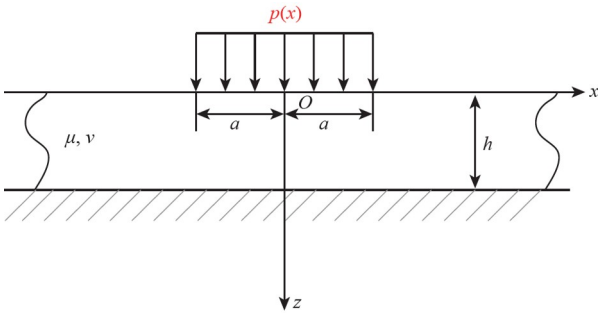

Figure 1 A finite elastic layer subjected to a uniform pressure.

shear strain, u_x and u_z are the displacement components in the direction x and z, respectively.

The constitutive relations can be readily expressed as

$$\begin{cases} \varepsilon_x = \dfrac{1}{2\mu}[\sigma_x - \nu(\sigma_x+\sigma_z)], \\ \varepsilon_z = \dfrac{1}{2\mu}[\sigma_z - \nu(\sigma_x+\sigma_z)], \\ \varepsilon_{xz} = \dfrac{\sigma_{xz}}{2\mu}, \end{cases} \tag{8}$$

where μ is the bulk shear modulus and ν is the Poisson's ratio.

Since assume a prefect bonding between an elastic layer and rigid substrate, the displacement boundary conditions are written as

$$u_x(x,h) = 0, \quad u_z(x,h) = 0, \tag{9}$$

In accordance with Eq. (5), the boundary conditions of stress on surface of elastic layer are achieved:

$$\begin{cases} \sigma_z(x,0) + p(x) = -\dfrac{\phi_0}{J_s} u_{z,xx}(x,0), \\ \sigma_{xz}(x,0) = \left[\dfrac{1}{J_s}\phi_{0,x} - \dfrac{\phi_0}{J_s^2}\right] u_{x,xx}(x,0). \end{cases} \tag{10}$$

Since the length parameter D_0 is much smaller than the finite layer's thickness, we have $\phi_0^{\text{chem}} \approx \phi_{0b}$. Generally, the Lagrangian surface energy density ϕ_0 is related to structure of crystal. In this paper, adopting a typical FCC metallic structure and taking the pressurized surface as a (100) one considering the same atom spacing in bond direction. Thus $m = 1$. The initial lattice lengths are $a_{01} = a_{02} = a_{0s}$ and the relaxation parameters are $\lambda_1 = \lambda_2 = \lambda$. The surface strains are $\varepsilon_{s1} = \varepsilon_{s2} = \varepsilon_x/2 = \varepsilon^*$ for a (100) surface [38]. Using the Taylor's expansion and ignoring the high-order strain terms, the Lagrangian surface-energy density ϕ_0 in Eq. (1) can be reduced as

$$\phi_0 \approx \phi_{0b} + \frac{\sqrt{2}E_b a_0}{8}\varepsilon_x^2\big|_{z=0}. \tag{11}$$

From Eq. (11), one can see that the layer's surface energy density is associated with the surface strain ε_x result from the external load. That is to say, under the external load, the layer's surface energy density ϕ_0 would vary from the contact region to the noncontact region due to the different surface deformation. However, ε_x is much smaller than 1 in the infinitesimal deformation condition. The influence of ε_x^2 on the surface energy density ϕ_0 can be reasonably neglected and the surface energy density ϕ_0 can be regarded as a constant, i.e., the bulk surface energy density ϕ_{0b}, in the following analysis. Then, considering Eqs. (10), (11) and $J_s = \lambda^2(1+\varepsilon_x/2)^2$ yields the simplified stress boundary conditions:

$$\begin{cases} \sigma_z(x,0) + p(x) = -\phi_{0b} u_{z,xx}(x,0), \\ \sigma_{xz}(x,0) = -\phi_{0b} u_{x,xx}(x,0). \end{cases} \tag{12}$$

3.2 General solutions

Generally, such an elastic problem is solved using Fourier transformation methods with Airy stress function Ψ. The Fourier transformation is as follows:

$$\begin{aligned} \widetilde{\Psi}(s,z) &= \int_{-\infty}^{\infty} \Psi(x,z)\mathrm{e}^{\mathrm{i}xs}\mathrm{d}x, \\ \Psi(x,z) &= \frac{1}{2\pi}\int_{-\infty}^{\infty} \widetilde{\Psi}(s,z)\mathrm{e}^{-\mathrm{i}xs}\mathrm{d}s, \end{aligned} \tag{13}$$

and $\widetilde{\Psi}(s,z)$ can be written as

$$\widetilde{\Psi}(s,z) = (A+Bz)\mathrm{e}^{-|s|z} + (C+Dz)\mathrm{e}^{|s|z}, \tag{14}$$

where A, B, C and D are coefficient functions of s and h, which are defined by the stress boundary conditions in Eq. (12).

Thus, the integral form of the stresses and displacements are

$$\begin{cases} \sigma_x = \dfrac{\partial^2 \Psi(x,z)}{\partial z^2} = \dfrac{1}{2\pi}\displaystyle\int_{-\infty}^{\infty} \frac{\partial^2 \widetilde{\Psi}(s,z)}{\partial z^2}\mathrm{e}^{-\mathrm{i}sx}\mathrm{d}s, \\ \sigma_z = \dfrac{\partial^2 \Psi(x,z)}{\partial x^2} = -\dfrac{1}{2\pi}\displaystyle\int_{-\infty}^{\infty} s^2\widetilde{\Psi}(s,z)\mathrm{e}^{-\mathrm{i}sx}\mathrm{d}s, \\ \sigma_{xz} = -\dfrac{\partial^2 \Psi(x,z)}{\partial x \partial z} = \dfrac{1}{2\pi}\displaystyle\int_{-\infty}^{\infty} \mathrm{i}s\frac{\partial \widetilde{\Psi}(s,z)}{\partial z}\mathrm{e}^{-\mathrm{i}sx}\mathrm{d}s, \end{cases} \tag{15}$$

and

$$\begin{cases} u_x = -\dfrac{1}{2\sqrt{2}\pi\mu}\displaystyle\int_{-\infty}^{\infty}\left[(1-\nu)\frac{\partial^2 \widetilde{\Psi}(s,z)}{\partial z^2} + \nu s^2 \widetilde{\Psi}(s,z)\right] \\ \qquad \cdot \dfrac{\mathrm{e}^{-\mathrm{i}sx}}{s}\mathrm{d}s + X_1, \\ u_z = -\dfrac{1}{2\sqrt{2}\pi\mu}\displaystyle\int_{-\infty}^{\infty}\left[(1-\nu)\frac{\partial^3 \widetilde{\Psi}(s,z)}{\partial z^3} + (2-\nu)s^2\frac{\partial \widetilde{\Psi}(s,z)}{\partial z}\right] \\ \qquad \cdot \dfrac{\mathrm{e}^{-\mathrm{i}sx}}{s^2}\mathrm{d}s + X_2, \end{cases} \tag{16}$$

where X_1 and X_2 are the integral constants.

Substituting Eqs. (15) and (16) into Eqs. (9) and (12) leads to four linear equations. Solving the linear equations yields

$$A = \frac{\widetilde{p}(s)}{F}A_p, \quad B = \frac{\widetilde{p}(s)}{F}B_p, \quad C = \frac{\widetilde{p}(s)}{F}C_p, \quad D = \frac{\widetilde{p}(s)}{F}D_p, \tag{17}$$

where

$$\begin{cases} A_p = A_1\mathrm{e}^{2h|s|} + A_2 s^2 h^2 + A_3 h|s| + A_4, \\ B_p = |s|\left(B_1\mathrm{e}^{2h|s|} + B_2 s^2 h^2 + B_3 h|s| + B_4\right), \\ C_p = C_1\mathrm{e}^{-2h|s|} + C_2 s^2 h^2 + C_3 h|s| + C_4, \\ D_p = |s|\left(D_1\mathrm{e}^{-2h|s|} + D_2 s^2 h^2 + D_3 h|s| + D_4\right), \\ F = s^2\left[n_1\cosh(2h|s|) + n_2\sinh(2h|s|) + n_3\right]. \end{cases} \tag{18}$$

The detailed expressions of A_i, B_i, C_i, D_i (i = 1, 2, 3, 4) and n_j (j = 1, 2, 3) are presented in Appendix A. $\widetilde{p}(s)$ is the Fourier transformation form:

$$\widetilde{p}(s)=\frac{1}{2\pi}\int_{-\infty}^{\infty}p(x)\mathrm{e}^{\mathrm{i}xs}\mathrm{d}x. \tag{19}$$

The integral constants X_1 and X_2 in Eq. (16) can be defined by the displacement boundary conditions. In Fig. 1, as $p(x)$ is symmetric to the z-axis, we can define $u_x(0,z)=0$. Furthermore, by the Saint-Venant's principle, we define $u_z(r_0a,0)=0$, where r_0 is a finite value ($r_0\geqslant 5$) [31]. In this paper, we take $r_0=5$. Based on Eqs. (15) and (16), the solutions on the loading surface ($z=0$) can be obtained with the determined A, B, C, and D in Eq. (17).

$$\begin{aligned}
\sigma_x(x,0)&=\sqrt{\frac{2}{\pi}}\int_0^{\infty}\frac{-4\left\{\left[2h^2s^2-2hs^2l(1+\Lambda_1)-\Lambda_3-2\right]+\Lambda_2\cosh(2hs)+l\Lambda_2(1+\Lambda_1)s\sinh(2hs)\right\}\cos(sx)\widetilde{p}(s)}{2h^2s^2(l^2s^2-4)+l^2s^2\Lambda_2^2+4\Lambda_3+\Lambda_2\left(4-l^2s^2\Lambda_2\right)\cosh(2hs)-8l\Lambda_1\Lambda_2s\sinh(2hs)}\mathrm{d}s,\\
\sigma_z(x,0)&=\sqrt{\frac{2}{\pi}}\int_0^{\infty}\frac{-4\left[\left(-2h^2s^2+2hls^2\Lambda_1+\Lambda_3\right)+\Lambda_2\cosh(2hs)-l\Lambda_1\Lambda_2s\sinh(2hs)\right]\cos(sx)\widetilde{p}(s)}{2h^2s^2(l^2s^2-4)+l^2s^2\Lambda_2^2+4\Lambda_3+\Lambda_2\left(4-l^2s^2\Lambda_2\right)\cosh(2hs)-8l\Lambda_1\Lambda_2s\sinh(2hs)}\mathrm{d}s,\\
\sigma_{xz}(x,0)&=\sqrt{\frac{2}{\pi}}\int_0^{\infty}\frac{-2ls\left[-2h^2s^2-\Lambda_2(2\Lambda_1+1)+\Lambda_2(2\Lambda_1+1)\cosh(2hs)\right]\sin(sx)\widetilde{p}(s)}{2h^2s^2(l^2s^2-4)+l^2s^2\Lambda_2^2+4\Lambda_3+\Lambda_2\left(4-l^2s^2\Lambda_2\right)\cosh(2hs)-8l\Lambda_1\Lambda_2s\sinh(2hs)}\mathrm{d}s,
\end{aligned} \tag{20}$$

and

$$\begin{aligned}
u_x(x,0)&=\frac{-4}{\sqrt{2\pi}\mu}\int_0^{\infty}\frac{\left[(2h^2s^2+2\Lambda_1-\Lambda_3)-\Lambda_2\Lambda_4\cosh(2hs)\right]\sin(sx)\widetilde{p}(s)}{s\left[2h^2s^2(l^2s^2-4)+l^2s^2\Lambda_2^2+4\Lambda_3+\Lambda_2\left(4-l^2s^2\Lambda_2\right)\cosh(2hs)-8l\Lambda_1\Lambda_2s\sinh(2hs)\right]}\mathrm{d}s,\\
u_z(x,0)&=\frac{2}{\sqrt{2\pi}\mu}\int_0^{\infty}\frac{s\left(-2h^2s^2l+8h\Lambda_1-l\Lambda_2^2\right)+l\Lambda_2^2s\cosh(2hs)+4\Lambda_1\Lambda_2\sinh(2hs)}{s\left[2h^2s^2(l^2s^2-4)+l^2s^2\Lambda_2^2+4\Lambda_3+\Lambda_2\left(4-l^2s^2\Lambda_2\right)\cosh(2hs)-8l\Lambda_1\Lambda_2s\sinh(2hs)\right]}\\
&\quad\times\left[\cos(sx)-\cos(sr_0a)\right]\widetilde{p}(s)\mathrm{d}s,
\end{aligned} \tag{21}$$

where l denotes an intrinsic length scale characterized the surface effect, which is the bulk surface energy density-to-shear modulus ratio, i.e., $l=\phi_{0b}/\mu$. In the classical solutions, the surface effect is not considered, i.e., without surface energy density, we have $l=0$.

4. Analytical solutions of the finite elastic layer

Two typical Boussinesq problems related to the model that a finite elastic layer is perfectly bonded to the rigid substrate are solved respectively, i.e., the model with a uniform pressure and a concentrated force.

4.1 Analytical solutions of the model under a concentrated force

Exerting a point force P at $x=0$, i.e., $2p_0a\to P$ as $a\to 0$. The first expression in Eq. (19) can be rewritten as

$$\widetilde{p}(s)=\frac{P}{\sqrt{2\pi}}. \tag{22}$$

Thus, substituting Eq. (22) into Eqs. (20) and (21) leads to the following stress and displacement components,

$$\begin{cases}
\sigma_x(x,0)=-\dfrac{4P}{\pi}\displaystyle\int_0^{\infty}\frac{\left\{\left[2h^2s^2-2hs^2l(1+\Lambda_1)-\Lambda_3-2\right]+\Lambda_2\cosh(2hs)+l\Lambda_2(1+\Lambda_1)s\sinh(2hs)\right\}\cos(sx)\widetilde{p}(s)}{2h^2s^2(l^2s^2-4)+l^2s^2\Lambda_2^2+4\Lambda_3+\Lambda_2\left(4-l^2s^2\Lambda_2\right)\cosh(2hs)-8l\Lambda_1\Lambda_2s\sinh(2hs)}\mathrm{d}s,\\
\sigma_z(x,0)=-\dfrac{4P}{\pi}\displaystyle\int_0^{\infty}\frac{\left[\left(-2h^2s^2+2hls^2\Lambda_1+\Lambda_3\right)+\Lambda_2\cosh(2hs)-l\Lambda_1\Lambda_2s\sinh(2hs)\right]\cos(sx)\widetilde{p}(s)}{2h^2s^2(l^2s^2-4)+l^2s^2\Lambda_2^2+4\Lambda_3+\Lambda_2\left(4-l^2s^2\Lambda_2\right)\cosh(2hs)-8l\Lambda_1\Lambda_2s\sinh(2hs)}\mathrm{d}s,\\
\sigma_{xz}(x,0)=-\dfrac{2P}{\pi}\displaystyle\int_0^{\infty}\frac{ls\left[-2h^2s^2-\Lambda_2(2\Lambda_1+1)+\Lambda_2(2\Lambda_1+1)\cosh(2hs)\right]\sin(sx)\widetilde{p}(s)}{2h^2s^2(l^2s^2-4)+l^2s^2\Lambda_2^2+4\Lambda_3+\Lambda_2\left(4-l^2s^2\Lambda_2\right)\cosh(2hs)-8l\Lambda_1\Lambda_2s\sinh(2hs)}\mathrm{d}s,
\end{cases} \tag{23}$$

and

$$\begin{cases} u_x(x,0) = \dfrac{-2P}{\pi\mu}\displaystyle\int_0^\infty \frac{\left[(2h^2s^2+2\Lambda_1-\Lambda_3)-\Lambda_2\Lambda_4\cosh(2hs)\right]\sin(sx)\widetilde{p}\,(s)}{s\left[2h^2s^2(l^2s^2-4)+l^2s^2\Lambda_2^2+4\Lambda_3+\Lambda_2\left(4-l^2s^2\Lambda_2\right)\cosh(2hs)-8l\Lambda_1\Lambda_2 s\sinh(2hs)\right]}\mathrm{d}s_1, \\ u_z(x,0) = \dfrac{P}{\pi\mu}\displaystyle\int_0^\infty \frac{s\left(-2h^2s^2l+8h\Lambda_1-l\Lambda_2^2\right)+l\Lambda_2^2 s\cosh(2hs)+4\Lambda_1\Lambda_2\sinh(2hs)}{s\left[2h^2s^2(l^2s^2-4)+l^2s^2\Lambda_2^2+4\Lambda_3+\Lambda_2\left(4-l^2s^2\Lambda_2\right)\cosh(2hs)-8l\Lambda_1\Lambda_2 s\sinh(2hs)\right]} \\ \qquad \times\left[\cos(sx)-\cos(sr_0a)\right]\widetilde{p}\,(s)\mathrm{d}s. \end{cases} \tag{24}$$

Let $s = t/f$, $x = x'f$, $z = z'f$, $l = l'f$, $h = h'f$, $f = P/(\pi\mu)$. For loading surface, i.e., $z = 0$, the stresses and displacements are rewritten as

$$\begin{cases} \sigma_x(x,0) = -4\mu\displaystyle\int_0^\infty \frac{\left\{\dfrac{4\left[2h'^2t^2-2h't^2l'(1+\Lambda_1)-2-\Lambda_3\right]}{\cosh(2h't)}+\Lambda_2+l't(\Lambda_1+1)\tanh(2h't)\right\}\cos(x't)}{\dfrac{2h'^2t^2(l'^2t^2-4)+4\Lambda_3+l't^2\Lambda_2^2}{\cosh(2h't)}+\Lambda_2(4-l'^2t^2\Lambda_2)-8l'\Lambda_1\Lambda_2 t\tanh(2h't)}\mathrm{d}t, \\ \sigma_z(x,0) = -4\mu\displaystyle\int_0^\infty \frac{\left[\dfrac{-2h'^2t^2+2h'l'\Lambda_1t^2+\Lambda_3}{\cosh(2h't)}+\Lambda_2-\Lambda_1\Lambda_2 l't\tanh(2h't)\right]\cos(x't)}{\dfrac{2h'^2t^2(l'^2t^2-4)+4\Lambda_3+l't^2\Lambda_2^2}{\cosh(2h't)}+\Lambda_2(4-l'^2t^2\Lambda_2)-8l'\Lambda_1\Lambda_2 t\tanh(2h't)}\mathrm{d}t, \\ \sigma_{xz}(x,0) = -2\mu\displaystyle\int_0^\infty \frac{l't\left[\dfrac{-2h'^2t^2-\Lambda_2(1+2\Lambda_1)}{\cosh(2h't)}+\Lambda_2(1+2\Lambda_1)\right]\sin(x't)}{\dfrac{2h'^2t^2(l'^2t^2-4)+4\Lambda_3+l't^2\Lambda_2^2}{\cosh(2h't)}+\Lambda_2(4-l'^2t^2\Lambda_2)-8l'\Lambda_1\Lambda_2 t\tanh(2h't)}\mathrm{d}t, \end{cases} \tag{25}$$

and

$$\begin{cases} u_x(x,0) = -2f\displaystyle\int_0^\infty \frac{\left[\dfrac{2h'^2t^2+2\Lambda_1-\Lambda_3}{\cosh(2h't)}-\Lambda_2\Lambda_4\right]\sin(x't)}{t\left[\dfrac{2h'^2t^2(l'^2t^2-4)+4\Lambda_3+l't^2\Lambda_2^2}{\cosh(2h't)}+\Lambda_2(4-l'^2t^2\Lambda_2)-8l'\Lambda_1\Lambda_2 t\tanh(2h't)\right]}\mathrm{d}t, \\ u_z(x,0) = f\displaystyle\int_0^\infty \frac{\left[\dfrac{t(-2h'^2t^2l'+8h'\Lambda_1-l'\Lambda_2^2)}{\sinh(2h't)}+l'\Lambda_2^2 t\coth(2h't)+4\Lambda_1\Lambda_2\right]\left[\cos(x't)-\cos(r_0t)\right]}{t\left[\dfrac{2h'^2t^2(l'^2t^2-4)+4\Lambda_3+l't^2\Lambda_2^2}{\sinh(2h't)}+\Lambda_2(4-l'^2t^2\Lambda_2)\coth(2h't)-8l'\Lambda_1\Lambda_2 t\right]}\mathrm{d}t. \end{cases} \tag{26}$$

4.2 Analytical solutions of the model under a uniform pressure

As Fig. 1, a uniform pressure is exerted to the layer. Let $p(x) = p_0$ and $h' = h/a$, $s = t/a$, $l' = l/a$, $z' = z/a$, $x' = x/a$. $p(x)$ can be transformed to the Fourier expression:

$$\widetilde{p}\,(s) = \sqrt{\frac{2}{\pi}}\frac{p_0 a\sin t}{t}. \tag{27}$$

Hence, the stress and displacement components on the loading surface ($z = 0$) can be reduced by substituting Eq. (27) into Eqs. (20) and (21),

$$
\begin{cases}
\sigma_x(x,0)=\dfrac{-2p_0}{\pi}\displaystyle\int_0^{\infty}\dfrac{4\sin(t)\left\{\dfrac{4\left[2h'^2t^2-2h't^2l'(1+\Lambda_1)-2-\Lambda_3\right]}{\cosh(2h't)}+\Lambda_2+l't(\Lambda_1+1)\tanh(2h't)\right\}\cos(x't)}{t\left\{\dfrac{2h'^2t^2(l'^2t^2-4)+4\Lambda_3+l't^2\Lambda_2^2}{\cosh(2h't)}+\Lambda_2(4-l'^2t^2\Lambda_2)-8l'\Lambda_1\Lambda_2t\tanh(2h't)\right\}}\mathrm{d}t,\\
\sigma_z(x,0)=\dfrac{-2p_0}{\pi}\displaystyle\int_0^{\infty}\dfrac{4\sin(t)\left\{\dfrac{-2h'^2t^2+2h'l'\Lambda_1t^2+\Lambda_3}{\cosh(2h't)}+\Lambda_2-\Lambda_1\Lambda_2l't\tanh(2h't)\right\}\cos(x't)}{t\left\{\dfrac{2h'^2t^2(l'^2t^2-4)+4\Lambda_3+l't^2\Lambda_2^2}{\cosh(2h't)}+\Lambda_2(4-l'^2t^2\Lambda_2)-8l'\Lambda_1\Lambda_2t\tanh(2h't)\right\}}\mathrm{d}t,\\
\sigma_{xz}(x,0)=\dfrac{-2p_0}{\pi}\displaystyle\int_0^{\infty}\dfrac{2l't\sin(t)\left\{\dfrac{-2h'^2t^2-\Lambda_2(1+2\Lambda_1)}{\cosh(2h't)}+\Lambda_2(1+2\Lambda_1)\right\}\sin(x't)}{t\left\{\dfrac{2h'^2t^2(l'^2t^2-4)+4\Lambda_3+l't^2\Lambda_2^2}{\cosh(2h't)}+\Lambda_2(4-l'^2t^2\Lambda_2)-8l'\Lambda_1\Lambda_2t\tanh(2h't)\right\}}\mathrm{d}t,
\end{cases}
\tag{28}
$$

and

$$
\begin{cases}
u_x(x,0)=\dfrac{p_0a}{\pi\mu}\displaystyle\int_0^{\infty}\dfrac{-4\sin(t)\left\{\dfrac{2h'^2t^2+2\Lambda_1-\Lambda_3}{\cosh(2h't)}-\Lambda_2\Lambda_4\right\}\sin(x't)}{t^2\left\{\dfrac{2h'^2t^2(l'^2t^2-4)+4\Lambda_3+l't^2\Lambda_2^2}{\cosh(2h't)}+\Lambda_2(4-l'^2t^2\Lambda_2)-8l'\Lambda_1\Lambda_2t\tanh(2h't)\right\}}\mathrm{d}t,\\
u_z(x,0)=\dfrac{p_0a}{\pi\mu}\displaystyle\int_0^{\infty}\dfrac{2t\sin(t)\left\{\dfrac{t(-2h'^2t^2l'+8h'\Lambda_1-l'\Lambda_2^2)}{\sinh(2h't)}+l'\Lambda_2{}^2t\coth(2h't)+4\Lambda_1\Lambda_2\right\}\left[\cos(x't)-\cos(r_0t)\right]}{t^2\left\{\dfrac{2h'^2t^2(l'^2t^2-4)+4\Lambda_3+l't^2\Lambda_2^2}{\sinh(2h't)}+\Lambda_2(4-l'^2t^2\Lambda_2)\coth(2h't)-8l'\Lambda_1\Lambda_2t\right\}}\mathrm{d}t.
\end{cases}
\tag{29}
$$

Consider the characteristics of the hyperbolic functions in Eqs. (28) and (29). When the elastic layer thickness approaches infinity, i.e., $h' \to \infty$, we have $\cosh(2h't) \to \infty$, $\sinh(2h't) \to \infty$, $\coth(2h't) \to 0$, $\tanh(2h't) \to 1$. The results can be well reduced to the ones of an elastic semi-infinite plane considering the surface effect [45]. Furthermore, while the value of contact width a greatly exceeds the intrinsic length l, i.e., the dimensionless quantity $l' \to 0$, the results can well degenerate to the classical ones [52].

5. Results and discussion

The stress and displacement solutions to the Boussinesq problem of a two-dimensionally finite elastic layer with surface effect are given as above. Here, analysis of the results under a uniform pressure is carried out since the case of a concentrated force is a special one. In the analysis below, we take $\nu = 0.37$.

The distributions of both the normal displacement u_z and the horizontal displacement u_x on a finite elastic layer surface are shown in Fig. 2 for cases with different l/a, in which the layer thickness is large enough ($h/a = 1000$) and the solutions for a half plane with surface effect [45] are also given for comparison. Different values of l/a denotes the degree of surface effect and $l/a = 0$ corresponds to the classical solution. From Fig. 2, it is discovered that the surface effect reduces both the horizontal displacement u_x and the normal displacement u_z, and the results of the finite elastic layer and those of the half plane [45] exhibit no obvious deviation. It means that the surface effect can harden the elastic layer, and the solutions about a semi-infinite plane can represent those of a finite elastic layer when the thickness value of layer is sufficiently large. The

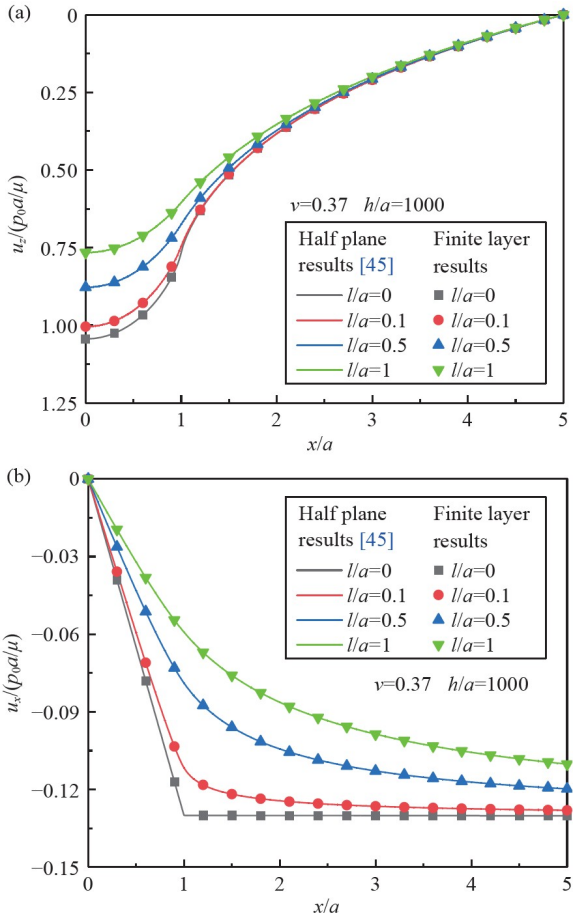

Figure 2 Dimensionless displacements on the surface of a finite elastic layer under a uniform pressure varying with the dimensionless parameter l/a. (a) The normal displacement u_z; (b) the horizontal displacement u_x.

stronger the surface effect, the harder the material becomes, and the smaller the displacements in the loading zone are. Furthermore, unlike the classical solution, there is a continuous slope for the horizontal displacement u_x, which is resulted from the continuous condition of surface effect.

The corresponding stresses on the surface of the elastic layer are illustrated in Fig. 3, where Fig. 3(a)-(c) exhibits the normal stresses σ_z, σ_x and the shear stress σ_{xz}, respectively. Additionally, the stress solutions to a half plane with the surface effect [45] are provided for comparison. $l/a = 0$ corresponds to the classic solution without the surface effect. It is found that, in the classical predictions, both σ_z and σ_x are uniform and compressive in the loading region and vanish outside the loading region. Both σ_z and σ_x are discontinuous at $x/a = 1$ due to the discontinuous boundary conditions at this point. When the surface effect is considered, both $|\sigma_z|$ and $|\sigma_x|$ decrease, in contrast to the classical ones in the loading region of $x/a \leqslant 1$; while both σ_z and σ_x are compressive outside the loading region, and become continuous and smooth at $x/a = 1$. All these are attributable to the surface effect, which introduces additionally surface-

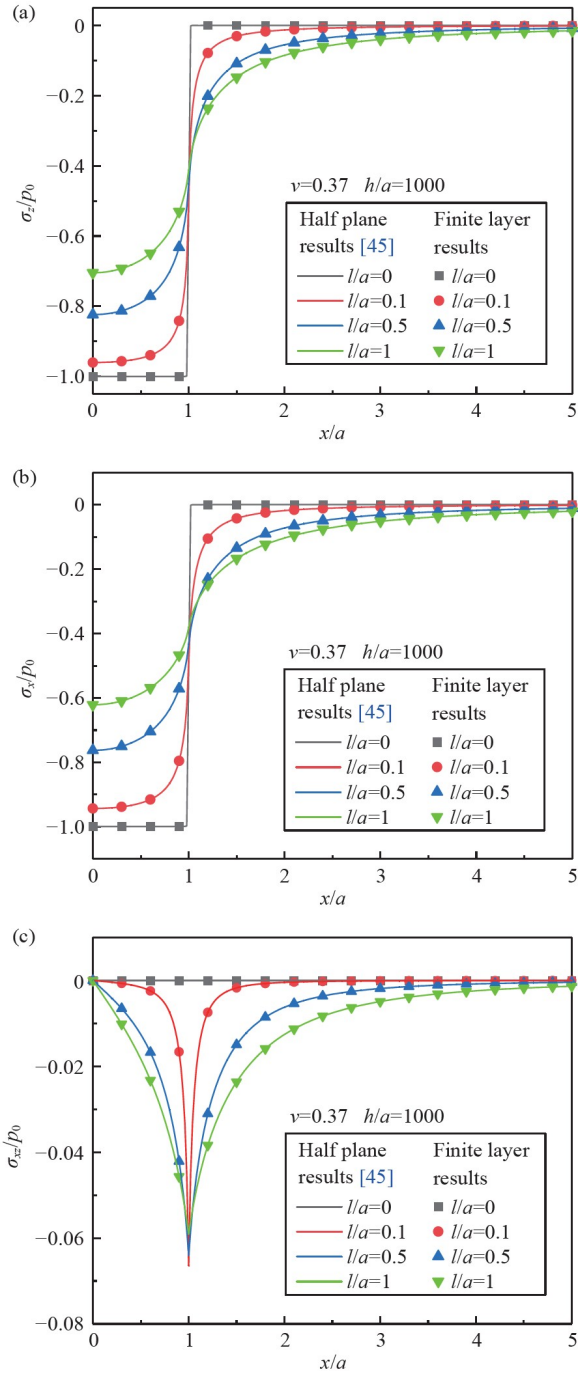

Figure 3 Dimensionless stresses on the surface of a finite elastic layer under a uniform pressure varying with the dimensionless parameter l/a. (a) The normal stress σ_z; (b) the normal stress σ_x; (c) the shear stress σ_{xz}.

induced normal and tangential tractions shown in Eq. (4). With regard to the shear stress illustrated in Fig. 3(c), it vanishes in the classical solution, while a non-vanishing shear stress exists when the surface effect is considered. The non-vanishing shear stress should be resulted from introduced surface-induced tangential traction, i.e., the third equation in Eq. (4). Furthermore, as l/a increases, a more notable deviation is observed between the present results

and the classical ones, suggesting that a stronger surface effect results in greater hardness of the elastic layer. Obviously, the solutions of an elastic half plane [45] can well represent those of a finite elastic layer when the layer is adequately thick.

The thickness effect of an elastic layer on the Boussinesq solutions is further investigated. Both the normal displacement u_z and the horizontal displacement u_x on a finite elastic layer are given in Fig. 4(a) and (b), respectively, for varying layer thicknesses, with or without the surface effect. Figure 4(a) illustrates a decrease in normal displacement u_z with the decreasing layer thickness, either with or without the surface effect, both of which are due to the rigid substrate effect, significantly resisting the elastic layer deformation. In comparison to the absence of the surface effect, the surface effect would lead to a decreased normal displacement in the loading region, an increased one however outside the loading region, resulting in a more uniform distribution of the normal displacement u_z. Specifically, In the event of a very thin elastic layer where the surface effect is not taken into account, for example $h/a = 2$, one can see that the pile-up phenomenon emerges outside the loading region, while the surface effect would decrease the pile-up deformation, which further proves the hardening behavior induced by the surface effect.

Similar hardening behavior can be found in the horizontal displacement as shown in Fig. 4(b), which further leads to the more uniform distribution of the horizontal displacement, in comparison with the result without the surface effect. Either with or without the surface effect, it is discovered that the horizontal displacement $|u_x|$ typically decreases as the elastic layer thickness decreases and the curve of the horizontal displacement changes from concave in the loading region to convex outside the loading region. Specially, in the case with a much small thickness, for example $h/a = 2$, one can see that the horizontal displacement changes its direction. Such a phenomenon in the case of a finite elastic layer is a result of the constraint effect of the rigid substrate. Squeezing in the thickness direction leads to the outward deformation in both the normal and horizontal directions outside the loading region.

The distributions of stresses on the finite elastic layer surface are illustrated in Fig. 5, where both the solutions with and without the surface effect are included for comparison. From Fig. 5(a), one can see that the dimensionless classical solution of the normal stress σ_z is not influenced by the layer thickness. σ_z is uniformly distributed inside the loading region and vanishes outside the loading region, which coincides with the classical boundary condition. In comparison to the classical solutions, the surface effect reduces the value of $|\sigma_z|$ inside the loading region result from the opposite direction of the surface-induced traction to that

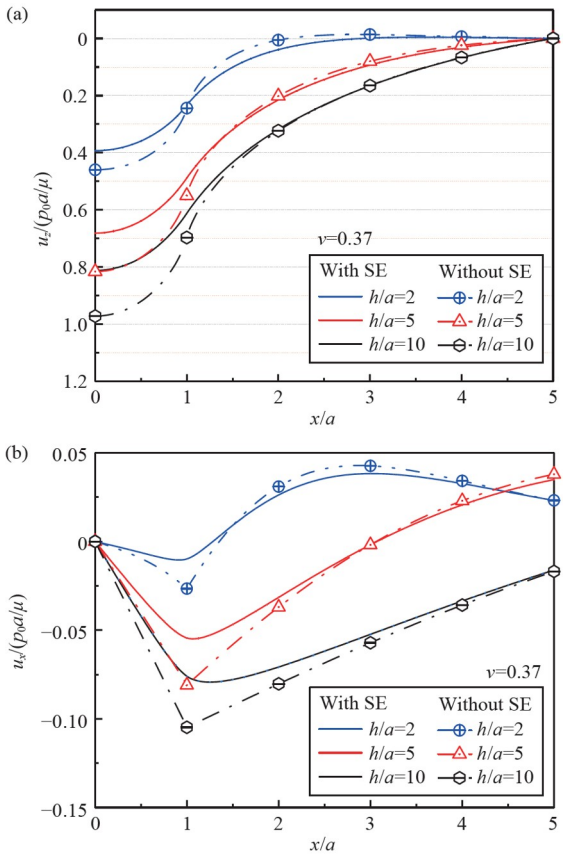

Figure 4 Dimensionless surface displacements of a finite elastic layer under a uniform pressure varying with the layer thickness, in which $l/a = 0.1$ is adopted for the surface effect and SE denotes "surface effect". (a) The normal displacement u_z; (b) the horizontal displacement u_x.

of the external loading. Outside the loading region, σ_z exists as a result of the surface effect. The direction of normal traction induced by surface inside the loading region should be opposite to that outside the loading region, which is due to the opposite deformation curvatures in the two regions shown in Fig. 4(a). Furthermore, the decreasing layer thickness yields an increasing value of $|\sigma_z|$ inside the loading region, which is owing to the resistance of the rigid substrate, like the nano-indentation problem of the film/substrate system [53]. Outside the loading region, the normal stress $|\sigma_z|$ hardly changes with the thickness due to a similar deformation curvature in this region.

The dimensionless normal stress $|\sigma_x|$ on the finite elastic layer surface is given in Fig. 5(b). In the model without considering the surface effect, the normal stress $|\sigma_x|$ decreases with the decreasing layer thickness and changes from a nearly uniform distribution to a non-uniform one in the loading region. Outside the loading region, σ_x changes from positive to zero, even negative in the thinner layer case. All these should be attributed to the rigid substrate effect, which can be understood from the horizontal dis-

placement shown in Fig. 4(b). When factoring in the surface effect, both the substrate effect and the surface effect will contribute to the results. Due to the surface effect-induced hardening behavior, the normal stress $|\sigma_x|$ will become smaller and distribute more uniformly in Fig. 5(b).

The dimensionless shear stress near the elastic layer surface is shown in Fig. 5(c). The shear stress σ_{xz} is zero when the surface effect is omitted from consideration, which actually corresponds to the boundary conditions. However, considering the surface effect, the shear stress σ_{xz} exists and changes directions along the horizontal direction. It is responsible for the surface-induced tangential traction, and the direction of the traction depends on that of the deformation curvature.

Though it is a Boussinesq problem of a finite elastic layer analyzed in the present paper, so as to illustrate the coupling surface and thickness effects, similar to Ref. [45], a generalized hardness of the finite elastic layer is defined as

$$H=\frac{2p_0a}{u_z(0,0)}=2\pi\mu\left\{\int_0^{\infty}\frac{2\sin(t)\left[t\left(\frac{-2h'^2t^2l'+8h'\Lambda_1-l'\Lambda_2^2}{\sinh(2h't)}+l'\Lambda_2^2t\coth(2h't)+4\Lambda_1\Lambda_2\right)\right]\left[\cos(x't)-\cos(r_0t)\right]}{t^2\left[\frac{2h'^2t^2\left(l'^2t^2-4\right)+4\Lambda_3+l't^2\Lambda_2^2}{\sinh(2h't)}+\Lambda_2(4-l'^2t^2\Lambda_2)\coth(2h't)-8l'\Lambda_1\Lambda_2t\right]}\mathrm{d}t\right\}^{-1}. \tag{30}$$

The normalized generalized hardness H/H_0 as a function of the ratio of a/l is shown in Fig. 6, where the half plane case and the finite layer case of different thicknesses are included. H_0 represents the generalized hardness of an elastic half plane predicted by the classical theory [54]. As Fig. 6 indicates, it is evident that the generalized hardness of an elastic half plane increases from 1 with the decreasing a/l, which is only due to the surface effect [45]. For a finite elastic layer, the normalized generalized hardness is larger than 1, which increases with the decreasing a/l as well as the decreasing thickness. Such a result exactly proves the coexistence of the thickness effect and the surface effect.

The results in Fig. 6 are qualitatively consistent with the experimental ones carried out by Ma et al. [55], in which a set of nanoindentation tests were done for the Ni/Fe substrate system with a Berkovich indenter. It is found that, for a small indentation depth, decreasing the indentation depth leads to an increase in the defined composite hardness, indicating an increasing hardness with the decrease of the contact radius.

Additionally, according to the G-M theory [12,13], Yuan and Wang [29] explored the nanocontact behavior of a finite elastic layer, taking into account the impact of surface tension, whose findings align qualitatively with the results of this research. Both findings suggest that the surface effect results in smoother normal stress distributions and a hardening layer. However, differences between them are inevitable due to the different surface constitutive equations and distinct material parameters that characterize the surface effect. In Ref. [29], the surface constitutive equations are given as a function of the surface stress and the surface effect is characterized only by the surface tension, whereas the surface elastic constant is neglected for simplicity. Consequently, only the normal surface-induced traction related to surface tension is considered in the stress boundary condition, leading to a vanishing shear stress on the loaded surface. Conversely, in the present work, the surface constitutive equations are expressed as a function of the surface energy density and the surface effect of the layer is delineated by the bulk surface energy density. Both additionally normal and tangential surface-induced tractions are introduced to the stress boundary condition as depicted in Eq. (12), which leads to a non-vanishing shear stress on the loaded surface.

Such a study provides a basic solution of the Boussinesq problem with the surface effect, which can be further extended to predict the nanoindentation hardness of layer/coating systems applied in various industries, for example, automobile body surface, turbine blade of aircraft, encapsulation layer of microelectronic devices, etc.

6. Conclusions

A two-dimensional Boussinesq problem of a finite elastic layer is explored in present paper, employing the surface elastic theory rooted in the surface energy density. Both the displacement and stress fields on the surface are achieved analytically by the Airy function and Fourier integral transformation methods in the circumstances of a concentrated force and a uniform pressure. It is observed that both the displacement and the stress on the surface are significantly influenced by not only the thickness effect but also the surface effect. An intrinsic length that characters the surface effect is defined by the bulk surface energy density and the bulk shear modulus. Surface effect would result in

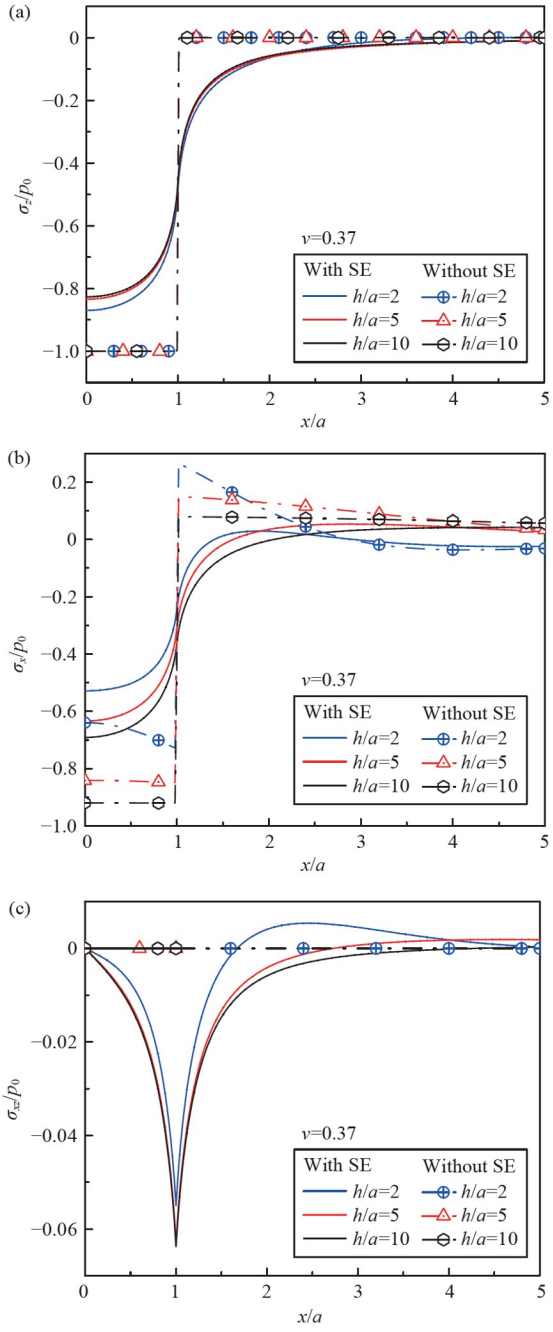

Figure 5 Dimensionless stresses on the surface of a finite elastic layer under a uniform pressure varying with the thickness, in which l/a = 0.1 is taken for the surface effect and SE denotes "surface effect". (a) The normal stress σ_z; (b) the normal stress σ_x; (c) the shear stress σ_{xz}.

the layer hardening. The larger the intrinsic length, the stronger the surface effect on the displacements and stresses is. Owing to the restriction of the rigid substrate, the thickness of the finite elastic layer influences the displacements and stresses also. The thinner the layer, the stronger the thickness effect is. When the layer thickness becomes thinner, the pile-up deformation due to the thickness effect in the classical solution could be decreased result from the

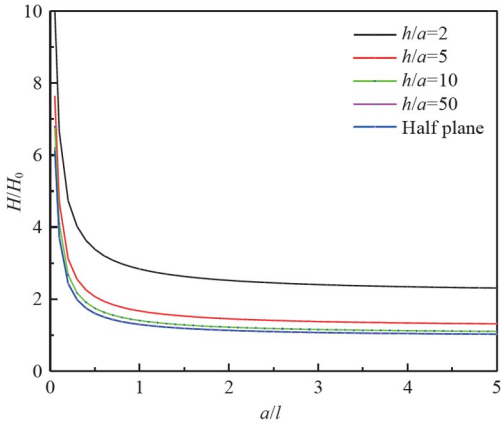

Figure 6 Variation of the normalized generalized hardness with respect to the dimensionless pressurized half-width for finite layers of different thicknesses.

surface effect. Both the surface effect and thickness effect can be included in a defined generalized hardness. The results may enrich the Boussinesq problem of a finite elastic layers, which should be useful for the design of advanced coatings and film-substrate systems.

Appendix A: Detailed expressions of the coefficients in Eq. (17)

$$\begin{cases} A_1 = 2\Lambda_2(-1 + l\Lambda_1|s|), \\ A_2 = -2(l|s| - 2), \\ A_3 = -4(1 + l\Lambda_1|s|), \\ A_4 = -2(\Lambda_3 + l\Lambda_1\Lambda_2|s|), \end{cases} \tag{A1}$$

$$\begin{cases} B_1 = -\Lambda_2(2 + l|s|), \\ B_2 = 0, \\ B_3 = 2(-2 + l|s|), \\ B_4 = l\Lambda_2|s| + 2, \end{cases} \tag{A2}$$

$$\begin{cases} C_1 = -2\Lambda_2(1 + l\Lambda_1|s|), \\ C_2 = 2(l|s| + 2), \\ C_3 = 4(1 - l\Lambda_1|s|), \\ C_4 = 2(-\Lambda_3 + l\Lambda_1\Lambda_2|s|), \end{cases} \tag{A3}$$

$$\begin{cases} D_1 = -\Lambda_2(-2 + l|s|), \\ D_2 = 0, \\ D_3 = -2(2 + l|s|), \\ D_4 = l\Lambda_2|s| - 2, \end{cases} \tag{A4}$$

$$\begin{cases} n_1 = \Lambda_2(-4 + \Lambda_2\xi^2 l^2), \\ n_2 = 8l\Lambda_1\Lambda_2|\xi|, \\ n_3 = -2\xi^2(-4 + l^2\xi^2)h^2 - l^2\Lambda_2^2\xi^2 - 4\Lambda_3, \end{cases} \tag{A5}$$

where $l=\frac{\phi_{0b}}{\mu}$, $\Lambda_1=-1+\nu$, $\Lambda_2=-3+4\nu$, $\Lambda_3=-5+12\nu-8\nu^2$, $\Lambda_4=-1+2\nu$.

Conflict of interest *On behalf of all authors, the corresponding author states that there is no conflict of interest.*

Author contributions *Hui Wu and Shaohua Chen designed the research. Hui Wu and Sha Xiao wrote the first draft of the manuscript. Zhilong Peng and Ning Jia helped organize the manuscript. Shaohua Chen and Ning Jia revised and edited the final version.*

Acknowledgements *This work was supported by the National Natural Science Foundation of China (Grant Nos. 12032004, 12293000, 12293002, and 12272043).*

1 D. M. Ebenstein, and L. A. Pruitt, Nanoindentation of biological materials, Nano Today **1**, 26 (2006).
2 T. M. Mayer, J. W. Elam, S. M. George, P. G. Kotula, and R. S. Goeke, Atomic-layer deposition of wear-resistant coatings for microelectromechanical devices, Appl. Phys. Lett. **82**, 2883 (2003).
3 R. C. Galan, F. Jimenez-Garrido, R. Dominguez-Castro, S. Espejo, T. Roska, C. Rekeczky, I. Petras, and A. Rodriguez-Vazquez, A bio-inspired two-layer mixed-signal flexible programmable chip for early vision, IEEE Trans. Neural Networks **14**, 1313 (2003).
4 Y. Cao, and Z. Xi, A review of MEMS inertial switches, Microsyst. Technol. **25**, 4405 (2019).
5 R. E. Miller, and V. B. Shenoy, Size-dependent elastic properties of nanosized structural elements, Nanotechnology **11**, 139 (2000).
6 G. F. Wang, and X. Q. Feng, Effects of surface stresses on contact problems at nanoscale, J. Appl. Phys. **101**, 013510 (2007).
7 P. Mohammadi, and P. Sharma, Atomistic elucidation of the effect of surface roughness on curvature-dependent surface energy, surface stress, and elasticity, Appl. Phys. Lett. **100**, 133110 (2012).
8 N. I. Tymiak, D. E. Kramer, D. F. Bahr, T. J. Wyrobek, and W. W. Gerberich, Plastic strain and strain gradients at very small indentation depths, Acta Mater. **49**, 1021 (2001).
9 W. X. Zhang, T. J. Wang, and X. Chen, Effect of surface/interface stress on the plastic deformation of nanoporous materials and nanocomposites, Int. J. Plast. **26**, 957 (2010).
10 J. R. Greer, W. C. Oliver, and W. D. Nix, Size dependence of mechanical properties of gold at the micron scale in the absence of strain gradients, Acta Mater. **53**, 1821 (2005).
11 V. S. Chandel, G. Wang, and M. Talha, Advances in modelling and analysis of nano structures: A review, Nanotechnol. Rev. **9**, 230 (2020).
12 M. E. Gurtin, and A. Ian Murdoch, A continuum theory of elastic material surfaces, Arch. Ration. Mech. Anal. **57**, 291 (1975).
13 M. E. Gurtin, and A. Ian Murdoch, Surface stress in solids, Int. J. Solids Struct. **14**, 431 (1978).
14 R. Dingreville, and J. Qu, Interfacial excess energy, excess stress and excess strain in elastic solids: Planar interfaces, J. Mech. Phys. Solids **56**, 1944 (2008).
15 D. J. Steigmann, and R. W. Ogden, Plane deformations of elastic solids with intrinsic boundary elasticity, Proc. R. Soc. Lond. A **453**, 853 (1997).
16 Z. P. Huang, and J. Wang, A theory of hyperelasticity of multi-phase media with surface/interface energy effect, Acta Mech. **182**, 195 (2006).
17 Z. Q. Wang, Y. P. Zhao, and Z. P. Huang, The effects of surface tension on the elastic properties of nano structures, Int. J. Eng. Sci. **48**, 140 (2010).
18 Y. Li, H. Zhang, X. Li, P. Shi, X. Feng, and S. Ding, Surface effects on the indentation of a soft layer on a rigid substrate with an elliptical cylinder indenter, Acta Mech. Sin. **38**, 422098 (2022).
19 S. Tirapat, T. Senjuntichai, J. Rungamornrat, and R. K. N. D. Rajapakse, Indentation of a nanolayer on a substrate by a rigid cylinder in adhesive contact, Acta Mech. **231**, 3235 (2020).
20 S. Dong, X. Fang, P. Yu, and J. Zhao, Surface effect induced thickness-dependent stress intensity factors of nano-thickness cracked metal plates, Eng. Fract. Mech. **261**, 108235 (2022).
21 J. Wang, Z. Huang, H. Duan, S. Yu, X. Feng, G. Wang, W. Zhang, and T. Wang, Surface stress effect in mechanics of nanostructured materials, Acta Mech. Solid Sin. **24**, 52 (2011).
22 Y. Xin, and J. Xiao, An analytic solution of an arbitrary location through-crack emanating from a nano-circular hole in one-dimensional hexagonal piezoelectric quasicrystals, Math. Mech. Solids **29**, 71 (2024).
23 Z. P. Huang, and L. Sun, Size-dependent effective properties of a heterogeneous material with interface energy effect: From finite deformation theory to infinitesimal strain analysis, Acta Mech. **190**, 151 (2007).
24 S. G. Mogilevskaya, S. L. Crouch, and H. K. Stolarski, Multiple interacting circular nano-inhomogeneities with surface/interface effects, J. Mech. Phys. Solids **56**, 2298 (2008).
25 P. Li, Q. Wang, and S. Shi, Differential scheme for the effective elastic properties of nano-particle composites with interface effect, Comput. Mater. Sci. **50**, 3230 (2011).
26 B. Paliwal, and M. Cherkaoui, Atomistic-continuum interphase model for effective properties of composite materials containing nano-inhomogeneities, Philos. Mag. **91**, 3905 (2011).
27 B. Paliwal, and M. Cherkaoui, Estimation of anisotropic elastic properties of nanocomposites using atomistic-continuum interphase model, Int. J. Solids Struct. **49**, 2424 (2012).
28 Y. Zhang, J. Cai, C. Mi, F. Wang, and A. H. Akbarzadeh, Effect of surface residual stress and surface layer stiffness on mechanical properties of nanowires, Acta Mech **233**, 233 (2022).
29 W. Yuan, and G. Wang, Cylindrical indentation of an elastic bonded layer with surface tension, Appl. Math. Model. **65**, 597 (2019).
30 X. Gao, F. Hao, D. Fang, and Z. Huang, Boussinesq problem with the surface effect and its application to contact mechanics at the nanoscale, Int. J. Solids Struct. **50**, 2620 (2013).
31 S. Zhou, and X. L. Gao, Solutions of half-space and half-plane contact problems based on surface elasticity, Z. Angew. Math. Phys. **64**, 145 (2013).
32 W. Zhou, and F. Yang, Effects of surface stress on the indentation response of an elastic half-space, Int. J. Mech. Sci. **229**, 107512 (2022).
33 J. Long, G. Wang, X. Q. Feng, and S. Yu, Effects of surface tension on the adhesive contact between a hard sphere and a soft substrate, Int. J. Solids Struct. **84**, 133 (2016).
34 X. J. Zhao, and R. K. N. D. Rajapakse, Analytical solutions for a surface-loaded isotropic elastic layer with surface energy effects, Int. J. Eng. Sci. **47**, 1433 (2009).
35 M. A. Attia, and F. F. Mahmoud, Analysis of nanoindentation of functionally graded layered bodies with surface elasticity, Int. J. Mech. Sci. **94-95**, 36 (2015).
36 J. Lawongkerd, T. M. Le, W. Wongviboonsin, S. Keawsawasvong, S. Limkatanyu, C. N. Van, and J. Rungamornrat, Elastic solution of surface loaded layer with couple and surface stress effects, Sci. Rep. **13**, 1033 (2023).
37 V. B. Shenoy, Atomistic calculations of elastic properties of metallic fcc crystal surfaces, Phys. Rev. B **71**, 094104 (2005).
38 S. Chen, and Y. Yao, Elastic theory of nanomaterials based on surface-energy density, J. Appl. Mech. **81**, 121002 (2014).
39 Y. Yao, and S. Chen, Surface effect on resonant properties of nanowires predicted by an elastic theory for nanomaterials, J. Appl. Phys. **118**, 044303 (2015).
40 L. Wang, H. Wu, and Z. Ou, Contact behaviors involving a nanobeam with surface effect by a rigid indenter, Math. Mech. Solids **29**, 401 (2024).
41 L. Wang, and H. Han, Vibration and buckling analysis of piezoelectric nanowires based on surface energy density, Acta Mech. Solid Sin. **34**,

425 (2021).
42 N. Jia, Y. Yao, Z. Peng, and S. Chen, Surface effect in nanoscale adhesive contact, J. Adh. **97**, 380 (2021).
43 N. Jia, Y. Yao, Y. Yang, and S. Chen, Analysis of two-dimensional contact problems considering surface effect, Int. J. Solids Struct. **125**, 172 (2017).
44 L. Wang, and Z. Ou, Modeling and analysis of the static bending of piezoelectric nanowires with the consideration of surface effects, J. Braz. Soc. Mech. Sci. Eng. **44**, 329 (2022).
45 L. Wang, Boussinesq problem with the surface effect based on surface energy density, Int. J. Mech. Mater. Des. **16**, 633 (2020).
46 L. Wang, L. Wang, H. Han, W. Han, and Y. Wang, Surface effects on nano-contact based on surface energy density, Arch. Appl. Mech. **91**, 4179 (2021).
47 R. J. K. Wood, Tribo-corrosion of coatings: A review, J. Phys. D-Appl. Phys. **40**, 5502 (2007).
48 H. A. Ching, D. Choudhury, M. J. Nine, and N. A. Abu Osman, Effects of surface coating on reducing friction and wear of orthopaedic implants, Sci. Tech. Adv. Mater. **15**, 014402 (2014).
49 V. J. Pauk, and C. Woźniak, Plane contact problem for a half-space with boundary imperfections, Int. J. Solids Struct. **36**, 3569 (1999).
50 X. Zhang, Q. J. Wang, Y. Wang, Z. Wang, H. Shen, and J. Liu, Contact involving a functionally graded elastic thin film and considering surface effects, Int. J. Solids Struct. **150**, 184 (2018).
51 P. Chhapadia, P. Mohammadi, and P. Sharma, Curvature-dependent surface energy and implications for nanostructures, J. Mech. Phys. Solids **59**, 2103 (2011).
52 G. Pickett, Stress distribution in a loaded soil with some rigid boundaries, Proc. High. Res. Bd. **18**, 35 (1939).
53 S. Chen, L. Liu, and T. Wang, Investigation of the mechanical properties of thin films by nanoindentation, considering the effects of thickness and different coating-substrate combinations, Surf. Coatings Tech. **191**, 25 (2015).
54 K. L. Johnson, Contact Mechanics (Cambridge University Press, Cambridge, 1987).
55 Z. S. Ma, Y. C. Zhou, S. G. Long, and C. Lu, On the intrinsic hardness of a metallic film/substrate system: Indentation size and substrate effects, Int. J. Plast. **34**, 1 (2012).

考虑表面效应的有限厚弹性层的Boussinesq问题

吴慧, 肖沙, 彭志龙, 贾宁, 陈少华

摘要 由于有限的厚度和较小的压痕尺寸, 厚度效应和表面效应对涂层的纳米压痕行为都有很重要的影响. 本文首先采用基于表面能密度的弹性理论研究了刚性基底上有限厚弹性层的二维Boussinesq问题. 利用艾里应力函数和傅里叶积分变换方法得到了该问题的基本解. 接着, 在集中力和均匀压力分别作用下, 得到了有限厚弹性层的应力场和位移场的解析解. 与经典解不同, 结果表明厚度效应和表面效应都会对Boussinesq弹性行为产生显著影响; 表面效应会使有限弹性层硬化, 并引起更均匀分布的位移场和应力场; 当厚度足够大时, 该问题退化为弹性半空间的Boussinesq解; 进一步定义了有限弹性层Boussinesq问题的广义硬度, 包含厚度效应和表面效应的耦合影响. 本研究将有助于涂层和具有层-基底结构的微器件的设计和性能评估.